JOURNAL OF MATERIALS SCIENCE 29 (1994) 2951–2956

Fractography of interlaminar fracture surfaces of CF/PI and CF/BMI composites

R. SELZER
Institute for Composite Materials Ltd, University of Kaiserslautern, 67663 Kaiserslautern, Germany
J. KREY
Du Pont de Nemours Deutschland GmbH, Du Pont Strasse 1, 61352 Bad Homburg, Germany

Interlaminar fracture is recognized as an important mode of failure of composite materials and structures. In order to characterize two *bis*maleinimide-matrix (BMI) composites and two polyimide-matrix (PI) composites regarding their delamination behaviour, interlaminar fracture tests in mode I, mode II and mixed-mode loading conditions were carried out. The aim of this study was to examine the fracture surfaces and to find relationships between features of the fracture surface and the corresponding mechanical data. The characteristic features of failure have been pointed out and the changes of the features with variations in matrix material, testing rate and loading mode have been shown. The results of the mechanical testing can be explained by means of SEM images.

1. Introduction

Interlaminar fracture is recognized as an important mode of failure of composite materials and structures. It can be the consequence of interlaminar defects that may be induced by low-energy impact or as a result of insufficient consolidation during the manufacturing of composite panels. Growth of these defects can occur under loading either in mode I (crack opening mode), mode II (forward shear mode) or a mixture of these conditions, as soon as a critical stress concentration at the interlaminar crack tip is exceeded. Because it is not possible to avoid such defects it is necessary to find composite materials with higher damage tolerance.

It is generally recognized that the interlaminar fracture toughness is dominated by the matrix phase. Therefore, the choice of matrix material is considered to be an important factor in the ultimate fracture properties of the laminate. It has been reported that the interlaminar fracture energy release rate increases with increasing matrix fracture energy [1, 2]. For this reason, new matrix systems were developed. While interlaminar failures have been studied extensively in the literature, little progress has been made towards developing an understanding of the micromechanisms of the failure processes.

The aim of this study was to examine fracture surfaces of double cantilever beam (DCB), end notched flexure (ENF) and end loaded split (ELS) samples and to find relationships between features of the fracture surface and the corresponding mechanical data. Images of fracture surfaces generated by similar conditions have been compared. The characteristic features of failure are pointed out and the changes of the features with variations in matrix material, testing rate and loading mode are shown.

2. Materials

In order to characterize two *bis*maleinimide-matrix (BMI) composites and two polyimide-matrix (PI) composites regarding their delamination behaviour, interlaminar fracture tests in mode I, mode II and mixed-mode loading conditions were carried out.

The two polyimide resins were provided by E. I. Du Pont Corporation, Wilmington, USA for composite applications under hot/wet conditions. Because resin A behaves in a rather brittle manner, resin B system was developed for improved damage tolerance [3]. The dry glass transition temperature, T_g, of composites with resin system A is about 250 °C and that for resin system B is 400 °C.

Carbon/*bis*maleinimide is a new class of composites with the matrix resin having moderately high glass transition temperatures, between 200 and 280 °C [4]. The two BMI-matrix composite systems were produced by BASF AG, Ludwigshafen, Germany. The BMI-matrix D is more brittle than C.

Du Ponts materials A and B and materials C and D of BASF are all reinforced with T 800 carbon fibres and have a 0°-fibre orientation.

Details of the materials investigated are given in Table I.

3. Test procedures and data reduction

In order to initiate delamination, a foil was placed at one end in the mid-thickness of the laminate during manufacturing. The specimens were loaded continuously in displacement control. Load and displacement were recorded throughout the test. All these tests were carried out following the recommendations of the

0022–2461

TABLE I Materials investigated

Producer	Material	Fibre	Matrix
Du Pont	A	T800 carbon fibre	PI matrix
	B	T800 carbon fibre	PI matrix (tougher than A)
BASF	C	T800 carbon fibre	BMI matrix 5250-4
	D	T800 carbon fibre	BMI matrix 5250-2 (brittle)

European Group on Fracture (EGF) for Standard Interlaminar Fracture Testing [5].

3.1. Mode I test

The specimen considered was parallel-sided with a width of 20 mm. Loading in the universal testing machine was introduced via machined loading blocks, which were glued to the specimen. Displacement rates of 0.5–50 mm min^{-1} were used in this study. The crack length was measured visually on the specimen edge, using a travelling microscope. A thin layer of white ink on the specimen edges facilitated this measurement. The crack tip propagation was noted every 5 mm in the diagram.

To calculate the critical energy release rate, G_{IC}, the corrected beam theory was used

$$G_{IC} = \frac{3P\delta}{2(a + \Delta)B} \quad (1)$$

where P is the force, δ the displacement, a the crack length, and B the specimen width. The corrected beam theory requires the determination of a correction factor, Δ, which takes crack-tip rotation and shear deformation into account. This correction is obtained by plotting the compliance to the one-third power, $C^{1/3}$, against crack length a. Δ is the intercept on the x-axis.

3.2. Mode II test

For the Mode II tests a specimen geometry (ENF) very similar to the Mode I specimen geometry (DCB) was used. Specimen width was 20 mm for these tests, too. In order to allow direct comparison of results, the distance between supports, $2L$, was fixed at 100 mm and the ratio of crack length to half span, a/h, was 0.5. The specimen was loaded in a standard three-point bending fixture at a crosshead rate of 0.5 mm min^{-1}. A travelling microscope was used to locate the crack tip at a predetermined position between the load nose and the outer support pin.

The values of G_{IIC} were calculated from experimental compliance method using the following expression

$$G_{IIC} = \frac{3m_2a^2P^2}{2B} \quad (2)$$

where m_2 is the slope of the plotted compliance versus the third power of crack length. The other parameters of this equation are explained in Equation 1.

3.3. Mixed-mode test

The typical specimen geometry for mixed mode tests (ELS) was identical to that used for the mode I DCB test. Generally, the free length was of the order of 100 mm, which allowed a reasonable crack propagation to take place, but large displacements should be avoided and the ratio of displacement/free length should be kept below 0.2.

The values of $G_{(I+II)C}$ were calculated from the experimental compliance method using the following expression

$$G_{(I+II)C} = \frac{3m_1a^2P^2}{2B} \quad (3)$$

where m_1 is the slope of the plotted compliance versus the third power of crack length. The other parameters of this equation are explained in Equation 1. Equation 3 gives the overall strain energy release rate, which may then be split into mode I and mode II components by assuming that the ratio $G_I/G_{II} = 4/3$.

3.4. Evaluation of the fracture surface

The mode I, mode II and mixed-mode specimens were cut for scanning electron microscope (SEM) investigation using a diamond saw. It was made certain that the fracture surfaces were neither damaged nor dirtied during this procedure. The fracture surface examination was carried out, after coating the fractured specimen with gold, in a Jeol JSM 5400 scanning electron microscope (SEM) using a secondary electron detector. In all SEM images the crack proceeded from the bottom-left to the top-right.

4. Results and discussion

4.1. Interlaminar fracture data

According to the testing procedures described above, the interlaminar fracture behaviour of the various carbon fibre-reinforced polymer composites has been investigated in previous works [3, 6]. The results of these studies are summarized in Fig. 1.

To examine the rate dependency of the fracture mechanism, the load–displacement behaviour was examined over a wide range of crosshead rates. The effect of the crosshead speed was investigated for

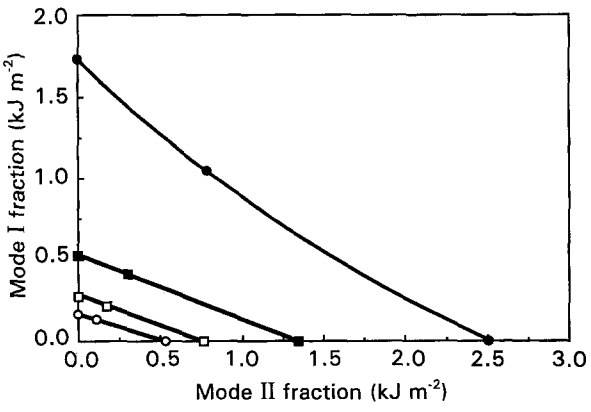

Figure 1 Results for all materials tested at low loading rates: material (■) A (Du Pont), (●) B (Du Pont), (□) C (BASF), (○) D (BASF).

mode I tests using three speeds: 0.5, 5 and 50 mm min^{-1}.

Fig. 2 shows toughness values plotted versus crack tip opening displacement rate on a semilog scale. This diagram shows the final values for G_{IC} at different displacement rates. The more brittle matrix materials exhibit no effect on the displacement rate, but a clear maximum is visible for the tough PI-matrix at a crosshead rate of $v = 5$ mm min^{-1} which corresponds to a crack tip displacement rate 10^{-9}–10^{-8} m s^{-1}. Gillespie *et al.* [7] obtained the same result for a brittle epoxy and a tough PEEK matrix composite material [7]. They explained the increase of G_{IC} by an increase of the plastic zone size at the crack tip because of a decreasing yield stress of the matrix with increasing displacement rate. The decrease of G_{IC} at higher strain rates is due to a time-dependent viscoelastic effect, which causes an energy-consuming crack process zone at low strain rates and disappears at high strain rates. Both effects are dominant only in ductile matrix materials such as the tough PI-matrix in this case.

4.2. Fractography

4.2.1. Effect of testing rate

Because the fracture surfaces of the specimens tested at $v = 0.5$ and 5 mm min^{-1} look very similar, only the surfaces of the specimen tested at 0.5 and 50 mm min^{-1} are compared with each other.

On all fracture surfaces many fibre fragments were found. The number of fibre fragments is independent of the crosshead rate. However, on surfaces produced at the low velocity, more matrix fragments were detected. The second difference to be recognized on the surfaces is that the fracture surface tested at 50 mm min^{-1} appears to be smoother than the other surfaces, on which larger differences in altitude can be found. The main difference between the surfaces tested with low velocity and with high velocity becomes obvious when comparing the surfaces at a higher magnification. Clearly, the matrix covers the fibre completely on the surface produced with a crosshead speed of 0.5 mm min^{-1} (Fig. 3). In contrast to this, the fibres of the 50 mm min^{-1} surface are nearly bare (Fig. 4). Comparing the fracture surfaces of the more brittle materials A, C and D the following statement can be made: the higher the testing rate, the worse becomes the fibre–matrix adhesion and the more brittle the matrix becomes. This statement cannot be verified for the tough PI-matrix material, because the fibres on all surfaces are torn out and are almost totally bare. It is not possible to find rate dependency of the fibre–matrix bonding of this material, because the fibre–matrix adhesion is poor at all testing rates.

On examining the surfaces of the tough material B it can be seen that all testing rates produce a rugged fracture surface with a lot of removed fibre bundles and fibre fragments (Fig. 5). Garg and Ishai [8] found

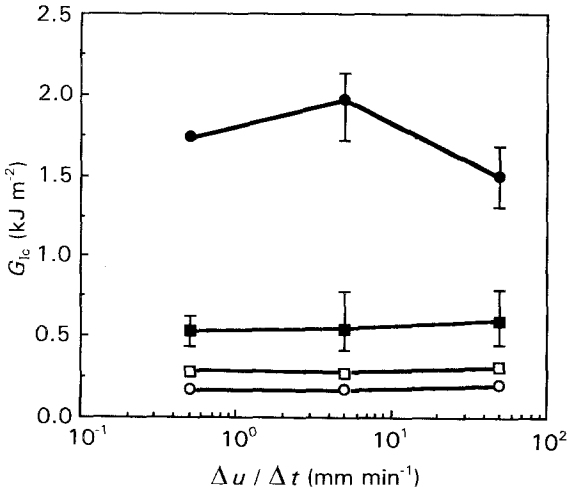

Figure 2 G_{IC} values for all materials tested at different loading rates. For key, see Fig. 1.

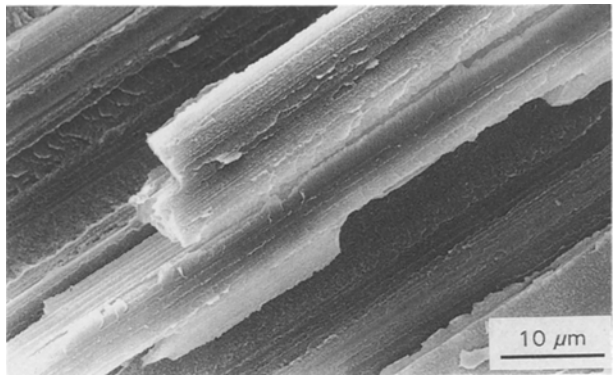

Figure 3 Mode I fracture surface of Du Pont Material A at low crosshead speed ($v = 0.5$ mm min^{-1}).

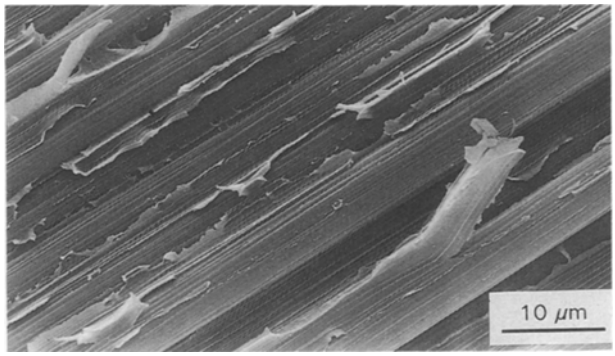

Figure 4 Mode I fracture surface of Du Pont Material A at high crosshead speed ($v = 50$ mm min^{-1}).

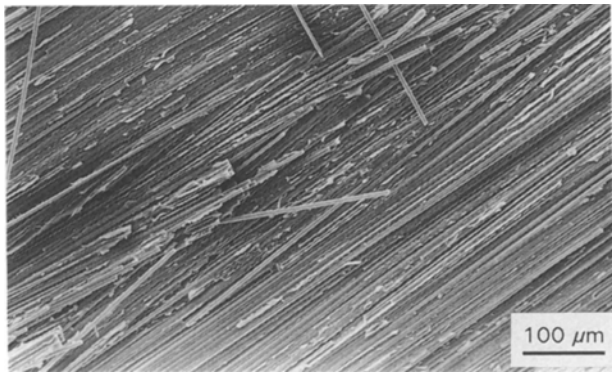

Figure 5 Mode I fracture surface of Du Pont Material B at high crosshead speed ($v = 50$ mm min^{-1}).

that the higher the surface roughness, the higher was the toughness of the composite, because more fibres were involved in the material's crack growth resistance. But this is not the only reason for such a high G_{IC} value. Another very important reason is that the fibres of materials A, C and D are generally confined to uniform layers, and thus the fracture produces a relatively flat fracture surface. With the tough material, on the other hand, the fibre layers are not well-defined, and the fibres from the various layers tend to intermingle. This feature, which has been termed nesting, makes it necessary to pull fibres out of the adjacent layers in order to propagate the crack. The propagation can occur in two ways. First the crack tip may bend around the fibres as it advances, thus loosing its planarity. This complicates the crack-tip stress field and leads to an increase in the fracture surface area that is not accounted for in the calculations. Secondly, some of the fibres may extend at an angle across the crack opening behind the crack tip. As the crack surfaces separate, these fibres must be either broken or pulled out of the fibre layers on one or both sides of the failure surface. This effect has been called fibre bridging. Both nesting and fibre bridging lead to a rough fracture surface and higher values for the apparent interlaminar G_{IC}. A similar result has been found by Hunston *et al.* [9] who investigated the influence of composite uniformity on fracture behaviour of thermoset and thermoplastic polymers reinforced with carbon fibres.

It is well known that the interlaminar fracture toughness depends on many factors. Some, which tend to increase the composite's fracture energy, are resin toughness, fibre-nesting and bridging as well as fibre breakage and pull-out during crack growth. Factors which tend to lower the interlaminar fracture energy include weak fibre–matrix bonding.

As a conclusion from the mechanical data and the fractographic results it can be stated that material B has the highest G_{IC} values at all testing rates. Reasons are the higher resin toughness and the other factors mentioned above, even though the fibre–matrix adhesion of this composite is rather poor. Therefore, a further capacity of increasing the G_{IC} value might be given by optimizing the fibre–matrix bond quality.

4.2.2. Loading mode effects

4.2.2.1. Mode I. Comparing the mode I fracture surfaces of all materials, typical mode I fracture features can be found. Many fibre and fibre-bundle fragments as well as broken fibre ends are on the surface as a result of the breakage of bridging fibres and fibre bundles.

The following features can be found on all materials compared:

(a) loose fibres and fibre bundles. These features are due to fibre or fibre bundles bridging the crack during propagation. The crack propagates and the fibres or bundles are torn out or peeled off their original layer. This is caused by nesting of fibres or crack plane jumping;

(b) fibre breakage. Fibres which are bridging a crack and cannot be peeled off their layer must break. Their ends can then be found in the opened fibre beds;

(c) fibre fragments. Pieces of broken fibres and fibre bundles are often lying on the surface. These pieces can be removed by blowing them away, in contrast to the broken fibre ends which are still embedded in the matrix.

Comparing the mode I fracture surfaces of the two PI-materials (Figs 6 and 7), the following features can be found: the fracture surface of material A is found to be rather smooth, whereas the surface of material B shows big differences in altitude. This is a result of the fact that the fibres in material A are lying parallel side by side, whereas in material B the fibres are lying in the matrix at an angle of about $\pm 10°$ relative to the original fracture plane. Comparing micrographs of both materials at higher magnifications it can be concluded that material A has a better fibre–matrix bonding than material B, but matrix B is tougher because it is more deformed than matrix A.

With regard to the loading mode effects in the case of the BASF materials, it can be mentioned that on the mode I fracture surfaces of both materials, pieces of broken fibres and fibre bundles are also found. The fracture surface of BASF material A is, however, not as plane as the surface of BASF material B. In addition, the mode I fracture surfaces of the BASF materials exhibit a brittle appearance, with bare fibres and a small degree of polymer deformation.

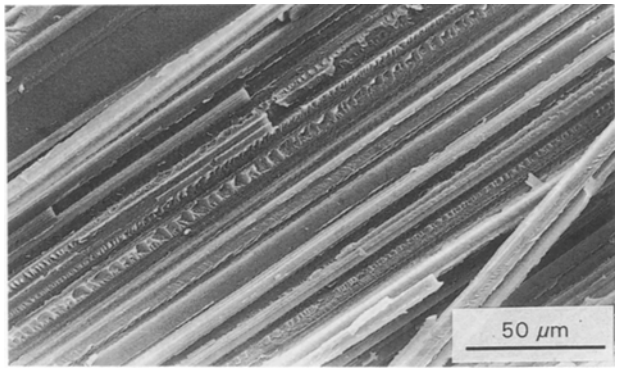

Figure 6 Mode I fracture surface of Du Pont Material A at low crosshead speed ($v = 0.5\ \text{mm min}^{-1}$).

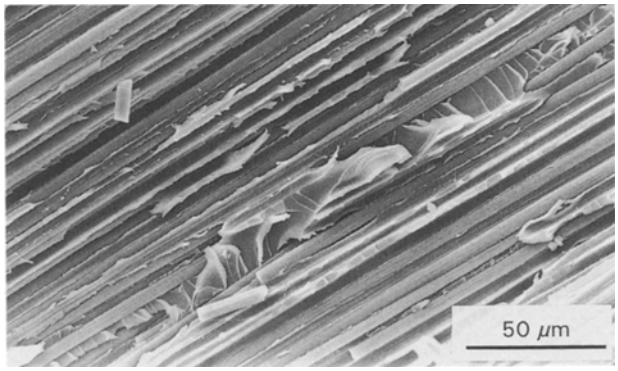

Figure 7 Mode I fracture surface of Du Pont Material B at low crosshead speed ($v = 0.5\ \text{mm min}^{-1}$).

4.2.2.2. Mode II. The two main differences between a mode I and a mode II fracture surface are that on the mode II fracture surfaces almost no fibre fragments and only a very few fibre breakage sites are detectable. The most important micro-fractographic characteristic of interlaminar fracture that occurs due to shear stresses is hackles. When shear stresses act between two laminate layers, initial damage in the form of microcracks occurs, due to local tensile stresses in the sheared region (Fig. 8a). The number of cracks occurring due to tensile stresses increases with growing shear stress (Fig. 8b). If these cracks reach the next fibre layer, the crack direction will turn (Fig. 8c). Final failure due to shear stresses occurs when all the individual cracks interconnect (Fig. 8d) [10].

The mode II fracture surfaces of the materials from Du Pont show the following differences relative to each other:

(a) at lower magnifications it can be seen that material A has a smooth fracture surface in contrast to material B, which shows big differences in altitude;

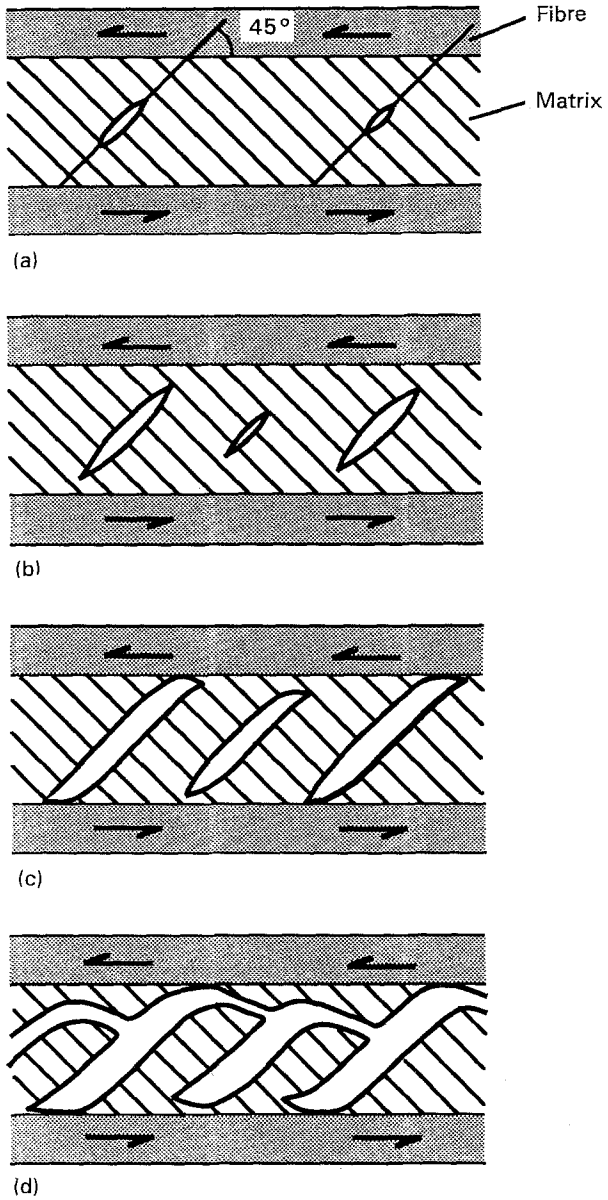

Figure 8 Origin of hackles (shear cusps) after [10].

(b) matrix pieces of material A adhere to the fibres, whereas fibres of material B look rather bare;

(c) only a few hackles are found on both fracture surfaces, but hackles of material B are more deformed (Figs 9 and 10).

Under mode II testing conditions, materials C and D behave in a similar manner, in producing a larger amount of hackles during unstable crack growth (Fig. 11) in contrast to stable crack growth (Fig. 12). Also both materials seem to have an improved fibre–matrix adhesion during unstable crack growth. On comparing these two materials, it was found that:

(a) fibre–matrix adhesion is worse for material C;

(b) hackles are more deformed in material C;

(c) the number of hackles is larger for material D.

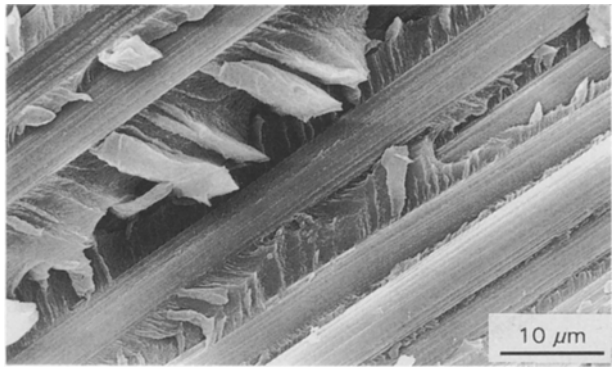

Figure 9 Mode II fracture surface of Du Pont Material A at low crosshead speed ($v = 0.5\ \text{mm min}^{-1}$).

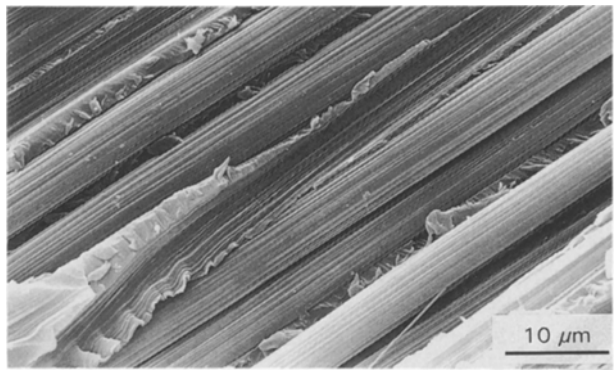

Figure 10 Mode I fracture surface of Du Pont Material B at low crosshead speed ($v = 0.5\ \text{mm min}^{-1}$).

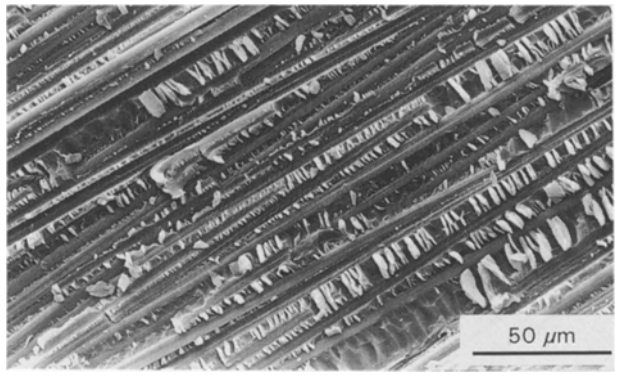

Figure 11 Mode II fracture surface of BASF Material D with unstable crack growth.

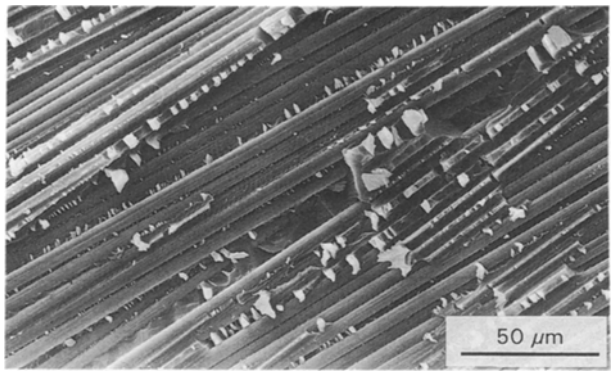

Figure 12 Mode II fracture surface of BASF Material D with stable crack growth.

4.2.2.3. Mixed mode. Mixed mode is a combination of mode I and mode II and the same is valid for the features on a mixed-mode fracture surface. Features of mode I and mode II fracture can be seen, depending on the mode which determined the crack propagation.

Like the other two fracture modes, the mixed-mode fracture surface of Du Ponts material A is very smooth and the surface of Du Ponts material B shows differences in altitude. Furthermore, there are more matrix pieces sticking to the fibres of material A while the fibres of material B are almost bare.

The mixed mode fracture surfaces of materials A and B show the following differences:

(a) there are very few loose fibres or fibre bundles on the surface of material A in contrast to the surface of material B;

(b) no hackles are found on the fracture surface of material A. On material B some structures are found which look like deformed hackles.

For the BASF materials in mixed mode, discrimination may again be made between stable and unstable crack growth. The following statements can be made for both materials. Stable crack growth causes very many deformed hackle-like structures. Hackles can clearly be detected on unstable crack growth fracture surfaces. In addition, during stable crack growth, fibre–matrix adhesion is improved because it is observed that on the corresponding fracture surfaces, more matrix still adheres to the fibres. Material C is set apart from material D during mixed-mode loading because fewer deformed matrix particles and hackles are found on the fracture surface.

5. Conclusions

The aim of this study was to examine fracture surfaces of DCB, ENF and ELS samples and to find relationships between features of the fracture surface and the corresponding mechanical data.

The fibre–matrix bonding of Du Pont material A is better than that of Du Pont material B because on fracture surfaces of material A only a few or even no detachments at all of matrix from the fibres are detected. Particles of matrix material still adhere to the fibres. Fibres of material B are often peeled off from the matrix. Material B matrix (Du Pont) seems to be more ductile than material A matrix (Du Pont) because it is more deformed after testing. This results in the highest fracture toughness value for Material B achieved in the test series discussed. Material D (BASF) has a stronger fibre–matrix bonding than material C (BASF). The matrix of material D is more ductile than the matrix of material C. The results of mechanical testing can be explained by means of SEM images.

Acknowledgements

The support of these studies, for example in the form of free material supply from BASF, Ludwigshafen, Germany, and Du Pont, Wilmington, USA, is gratefully acknowledged. Further thanks are due to the Volkswagen Foundation (AZ.: I66947) for their financial help to perform a study on the interlaminar fracture behaviour of polymer-based composites, and to Professor Friedrich's AGARD-Project G 75 (Post-failure Analysis of ILF). The authors also thank Professor K. Friedrich for discussions on this topic and for comments on the manuscript, and Dr D. L. G. Sturgeon for originally suggesting the research topic.

References

1. H. CHAI, *Int. J. Fract.* **43** (1990) 117.
2. R. W. LANG, M. HEYM, H. TESCH and H. STUTZ, in "High Tech – the way into the nineties", edited by K. Brunsch, H. -K. Gölden and C. -M. Herkert (Elsevier Science, Amsterdam, 1986) p. 261.
3. H. WITTICH, J. KREY and K. FRIEDRICH, *J. Mater. Sci. Lett.* **11** (1992) 1490.
4. H. WITTICH, private communications, University of Hamburg-Harburg, Germany (1993).
5. P. DAVIES, European Group on Fracture, Polymers and Composites Task Group, Interlaminar Fracture Testing of Composites (Ecole Polytechnique Fédérale de Lausanne, Switzerland, 1990).
6. H. WITTICH, K. FRIEDRICH, G. CHRISTOPOULOS and V. ALTSTÄDT, in "Proceedings of Fifth European Conference on Composites", edited by A. R. Bunsell, J. F. Jamet and A. Massiah (EACM, Bordeaux, 1992) p. 319.
7. J. W. GILLESPIE Jr, L. A. CARLSSON and A. J. SMILEY, *Compos. Sci. Technol.* **28** (1987) 1.
8. A. GARG and O. ISHAI, *Eng. Fract. Mech.* **22** (1985) 413.
9. D. L. HUNSTON, R. J. MOULTON, N. J. JOHNSTON and W. D. BASCOM, in "Toughened composites", ASTM STP 937, edited by N. J. Johnston (American Society for Testing and Materials, Philadelphia, PA, 1987) p. 74.
10. D. PURSLOW, *Composites* **17** (1986) 289.

Received 30 March
and accepted 24 November 1993